

INTAKE FLOW AND TIME STEP ANALYSIS IN THE MODELING OF A DIRECT INJECTION DIESEL ENGINE

Flavio V Zancanaro Jr, zancanaro@mecanica.ufrgs.br

Horácio A Vielmo, vielmoh@mecanica.ufrgs.br

Mechanical Engineering Department, Federal University of Rio Grande do Sul,
Rua Sarmento Leite, 425, CEP 90050-170, Porto Alegre, RS, Brazil.

Abstract. *This paper discusses the effects of the time step on turbulence flow structure in the intake and in-cylinder systems of a Diesel engine during the intake process, under the motored condition. The three-dimensional modeling of a reciprocating engine geometry comprising a bowl-in-piston combustion chamber, intake port of shallow ramp helical type and exhaust port of conventional type. The equations are numerically solved, including a transient analysis, valves and piston movements, for engine speed of 1500 rpm, using a commercial Finite Volumes CFD code. A parallel computation is employed. For the purpose of examining the in-cylinder turbulence characteristics two parameters are observed: the discharge coefficient and swirl ratio. This two parameters quantify the fluid flow characteristics inside cylinder in the intake stroke, therefore, it is very important their study and understanding. Additionally, the evolution of the discharge coefficient and swirl ratio, along crank angle, are correlated and compared, with the objective of clarifying the physical mechanisms. Regarding the turbulence, computations are performed with the Eddy Viscosity Model $k-\omega$ SST, in its Low-Reynolds approaches, with standard near wall treatment. The system of partial differential equations to be solved consists of the Reynolds-averaged compressible Navier-Stokes equations with the constitutive relations for an ideal gas, and using a segregated solution algorithm. The enthalpy equation is also solved. A moving hexahedral trimmed mesh independence study is presented. In the same way many convergence tests are performed, and a secure criterion established. The results of the pressure fields are shown in relation to vertical plane that passes through the valves. Areas of low pressure can be seen in the valve curtain region, due to strong jet flows. Also, it is possible to note divergences between the time steps, mainly for the smaller time step.*

Keywords: *Diesel engine, cold flow, CFD, moving mesh, turbulence model, time step.*

1. INTRODUCTION

With the exponentially increasing computational power of modern computers, multi-dimensional Computational Fluid Dynamics (CFD) has found more and more applications in internal combustion engines (ICE) research, design and development. Enhanced understandings of the physical processes of combustion and correspondingly improved numerical models and methods have both driven multi-dimensional CFD simulation tools from qualitative description towards quantitative prediction (Lakshminarayanan and Aghav, 2010). Therefore, powerful CFD codes are required to have the capability of predicting complex turbulent flows from engine developments and design in a reasonable time scale.

In-cylinder flows of diesel engines are typically compressible turbulent flows. Turbulence by itself remains one of the most complex fundamental problems of fluid dynamics. The complexity of in-cylinder flows is further increased due to transient swirling flows, considering the usual complexity of the geometry, the large turbulence spectra associated with the annular vortical jet after the intake valve, adding the compressible non-isothermal effects. The detailed understanding of the flow dynamics characteristics of intake, cylinder and exhaust flow of ICE is necessary for an efficient combustion process and related emissions to the environment. Therefore, a numerical approach could thus be an alternative due to the capability of CFD for in-cylinder flow predictions in recent 20 years. Gosman (1985) can be regarded as one of the pioneers in the application of CFD simulation to investigate in-cylinder flows. Since then tremendous improvements have been achieved in computational techniques in this field of study.

Based on the literature studied, several researchers have conducted research to calculate the complex flow in the cylinder and piston bowl (Aita *et al.*, 1991; Chen *et al.*, 1998; Kurniawan *et al.*, 2007). The in-cylinder flow is largely determined by the swirl and tumble motion during the intake stroke and the squish flow into and out of a piston bowl. It is known that a helical port is more effective than a tangential port to attain the required swirl ratio with minimum sacrifice in the volumetric efficiency (Tindal *et al.*, 1982; Huh *et al.*, 1995).

Bianchi *et al.* (2002a) and Bianchi and Fontanesi (2003), focusing on directed intake port types determine the discharge coefficient, including comparisons with experimental measurements. An even more challenging situation occurs in the presence of swirl generator inlet ports of ramp helical type, including the determination of the swirl ratio. With the growing availability of turbulence models and computational resources, many works make comparisons, regarding their capacity to reproduce experimental data and CPU time demanding.

The compared $k-\varepsilon$ linear and nonlinear (quadratic and cubic) eddy viscosity models (Bianchi *et al.*, 2002b) concluding that cubic stress-strain relation provided the best agreement with data, for those ICE three-dimensional flows considered. In another work, Bianchi *et al.* (2002a) investigated the High-Reynolds and Low-Reynolds near wall

approaches, both with a cubic relationship between Reynolds stresses and strains. It was concluded that the Low-Reynolds approach (boundary layer also discretized by the mesh), although increasing the computational effort, presented more ability to capture the details of the tested ICE intake flow.

In a typical steady flow condition, Baratta *et al.* (2008) compared the $k-\epsilon$ cubic, in its High-Reynolds and Low-Reynolds approaches, for fixed intake valve lifts steady state situations. Thought the results it was possible to note significant divergences between the turbulence models employed, mainly in the calculated swirl ratio.

The present paper focuses on a transient numerical analysis of the same Diesel engine (Fiat Research Center, 1982, 1983) analyzed in Baratta *et al.* (2008, 2009). Looking for more suitable time step, the $k-\omega$ SST, in its Low-Reynolds approach, in its compressible and non-isothermal approach, were compared, regarding mainly the discharge coefficient and swirl ratio.

2. CASE DESCRIPTION

The engine under investigation is of a four-stroke compression-ignition, direct-injection single cylinder (Fig. 1). It was derived from an automotive diesel engine at Fiat Research Center. The engine had a swirl generator inlet port of shallow ramp helical type (Fiat Research Center, 1982 ; Tindal *et al.*, 1982). It is coupled with a seat valve with an inner diameter of 31.5 mm, and outer diameter of 34.5 mm. The outlet port is a conventional one, with a valve of an inner diameter of 26.7 mm, and outer diameter of 29.5 mm. The cylinder bore is 79.5 mm, stroke 86 mm, and compression ratio 18:1. The maximum intake valve lift is 8.1 mm, opening at 355° (5° before TDC) and closing at 595° (55° after BDC). The maximum exhaust valve lift is 8.1 mm, opening at 125° (55° before BDC) and closing at 365° (5° after TDC).

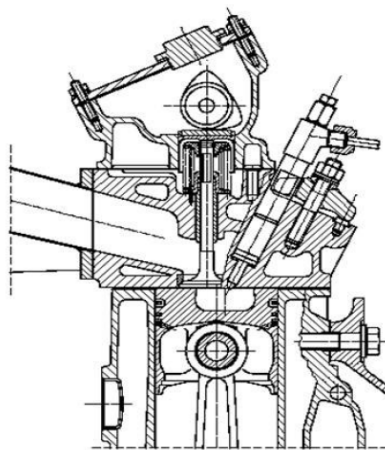


Figure 1. 1.9-L Fiat engine (Fiat Research Center, 1982; 1983)

2.1. Boundary and Initial Conditions

The boundary conditions are stagnation pressure (p_{st}) of 1 atm at the inlet, with 293.15 K, discharging in an ambient pressure (p_{out}) of 1 atm, and 293.15 K.

For all cases the turbulence boundary conditions are turbulence intensity $I = 0.05$, and length scale $l = 0.0035$ m, as a consequence of the flow and geometrical characteristics.

Regarding the heat transfer problem, considering a cold flow (exhaust and compression processes, without combustion), the cylinder wall and piston crown have a constant temperature of 400 K, and a thermal resistance of 0.004 m²K/W. For the combustion dome 450 K and 0.004 m²K/W. For the admission and exhaust valves and ports 350 K and 0.004 m²K/W.

As initial condition for the independency mesh analysis, the crankshaft starts at 320°, almost at the end of the exhaust process, followed by the valve crossing, and after the air admission. All the velocity components inside the cylinder are set 1 m/s, at 1 atm and 300 K. For the rest of the simulations, the initial conditions are the final fields of the previous cycle.

3. MATHEMATICAL MODEL

3.1. Governing Equations

The velocity field is described by the mass and momentum conservation equations (Navier-Stokes), in their transient, compressible form.

In Cartesian tensor notation, according Warsi (1981), the mass conservation is

$$\frac{\partial \rho}{\partial t} + \frac{\partial}{\partial x_j} (\rho u_j) = 0 \quad (1)$$

and the momentum

$$\frac{\partial \rho u_i}{\partial t} + \frac{\partial}{\partial x_j} (\rho u_j u_i - \tau_{ij}) = -\frac{\partial p}{\partial x_i} + s_i \quad (2)$$

where

$$p = p_s - \rho_0 g_m x_m \quad (3)$$

As the fluid is Newtonian, and the flow is turbulent, assuming the ensemble average (equivalent to time averages for steady-state situations), the stress tensor components are, according Hinze (1975),

$$\tau_{ij} = 2\mu S_{ij} - \frac{2}{3}\mu \frac{\partial u_k}{\partial x_k} \delta_{ij} - \overline{\rho u'_i u'_j} \quad (4)$$

and strain tensor

$$S_{ij} = \frac{1}{2} \left(\frac{\partial u_i}{\partial x_j} + \frac{\partial u_j}{\partial x_i} \right) \quad (5)$$

The u' are fluctuations about the ensemble average velocity, and overbar denotes the ensemble averaging process. Finally, as the flow is compressible and non-isothermal

$$s_i = g_i (\rho - \rho_0) \quad (6)$$

where g_i is the gravitational acceleration component in x_i direction. Considering the air as an ideal gas

$$\rho = \frac{p}{RT} \quad (7)$$

For the heat transfer problem, the enthalpy equation is also solved. According Jones (1980),

$$\frac{\partial \rho h}{\partial t} + \frac{\partial}{\partial x_j} (\rho h u_j + F_{h,j}) = \frac{\partial p}{\partial t} + u_j \frac{\partial p}{\partial x_j} + \tau_{ij} \frac{\partial u_i}{\partial x_j} \quad (8)$$

where $h = \bar{c}_p T - c_p^0 T_0$ is the static enthalpy; \bar{c}_p is the mean constant-pressure specific heat at temperature T ; c_p^0 the reference specific heat at temperature T_0 , and $F_{h,j}$ the diffusional energy flux in direction x_j , given by

$$F_{h,j} \equiv -k_t \frac{\partial T}{\partial x_j} + \overline{\rho u'_i h'} \quad (9)$$

where k_t is the thermal conductivity.

3.2. Governing Equations for the SST $k-\omega$ Model

The specific dissipation rate is defined as $\omega = \varepsilon / C_\mu k$, and the general form of the turbulent kinetic energy is

$$\frac{\partial}{\partial t} (\rho k) + \frac{\partial}{\partial x_j} \left[\rho u_j k - \left(\mu + \frac{\mu_t}{\sigma_k^\omega} \right) \frac{\partial k}{\partial x_j} \right] = \mu_t P - \rho \beta^* k \omega + \mu_t P_B \quad (10)$$

and specific dissipation rate is

$$\frac{\partial}{\partial t} (\rho \omega) + \frac{\partial}{\partial x_j} \left[\rho u_j \omega - \left(\mu + \frac{\mu_t}{\sigma_\omega^\omega} \right) \frac{\partial \omega}{\partial x_j} \right] = \alpha \frac{\omega}{k} \mu_t P - \rho \beta \omega^2 + \rho S_\omega + C_{\varepsilon 3} \mu_t P_B C_\mu \omega \quad (11)$$

where

$$P \equiv S_{ij} \frac{\partial u_i}{\partial x_j} \quad ; \quad P_B \equiv -\frac{g_i}{\sigma_{h,t}} \frac{1}{\rho} \frac{\partial \rho}{\partial x_i} \quad (12)$$

where $C_{\varepsilon 3}$ and C_{μ} are empirical coefficients. For $k-\omega$ SST model, the other coefficients are given in Menter (1993). In the SST $k-\omega$ model the turbulent viscosity is linked to k and ω via

$$\mu_t = \frac{a_1 k}{\max\left(a_1 \omega, \sqrt{\frac{1}{2} \Omega_{ij} \Omega_{ij}} F_2\right)} \quad (13)$$

4. NUMERICAL METHODOLOGY

Numerical transient solutions using a commercial Finite Volumes CFD code (Star-cd, 2008) were performed, for an engine speed (N) of 1500 rpm. A user defined unstructured hexahedral-trimmed cells moving mesh was constructed, as showed in the Fig. 2. A mesh independence study was performed, arriving in 1057084 cells in the cylinder, 352976 in the inlet port and 261996 in the exhaust port.

For the turbulence models applied, $k-\omega$ SST, in its Low-Reynolds approach, with standard near wall treatment. All computations were performed in double precision. The pressure-velocity coupling is solved thought the SIMPLE algorithm.

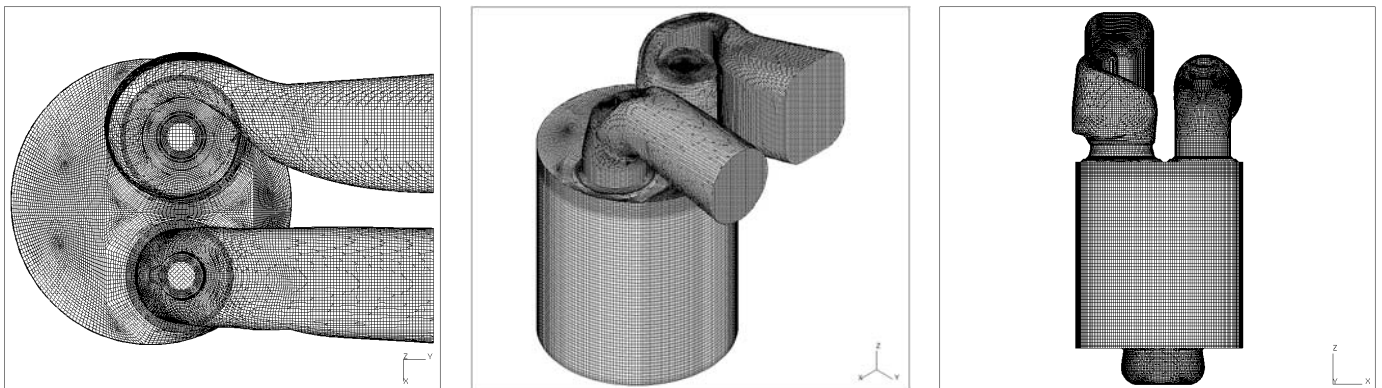


Figure 2. Unstructured hexahedral-trimmed cells moving mesh

By the complexity of the flow, aiming a stable solution, it was necessary to underrelax the momentum with 0.4, pressure 0.2, temperature 0.6, $k-\varepsilon-\omega$ 0.6, density 0.4, viscosity 0.4.

The time integration was made thought a fully implicit Euler scheme, with a constant time steps of 0.4° ($4.4444E-5$ s), 0.2° ($2.2222E-5$ s), 0.1° ($1.1111E-5$ s), and 0.05° ($5.5555E-6$ s) for a crank angular velocity of 1500 rpm.

The linear algebraic equations system was solved by the method of scalar preconditioned conjugate gradient.

As differencing schemes, were applied the Linear Upwind Differencing (LUD), according Wilkes and Thompson (1983), with blending factor (bf) of 0.3 for the momentum, turbulence and enthalpy equations. For the density the Central Differencing (CD) with bf = 0.3 (Hirsch, 2007).

5. THE DISCHARGE COEFFICIENT AND SWIRL RATIO

5.1. Discharge Coefficient

The discharge coefficient is a relation between the ideal and actual air mass flow rate that obtained in an isentropic expansion through the area $\pi d^2/4$. Therefore, the equation assumes the following form (Heywood, 1988 ; Ferrari, 2005),

$$C_D = \frac{\dot{m}_{actual}}{\dot{m}_{ideal}} = \frac{\dot{m}_{actual}}{\frac{\pi d^2}{4} \frac{P_{st}}{(RT)^{1/2}} \left(\frac{P_{out}}{P_{st}}\right)^{1/\gamma} \left\{ \frac{2\gamma}{\gamma-1} \left[1 - \left(\frac{P_{out}}{P_{st}}\right)^{(\gamma-1)/\gamma} \right] \right\}^{1/2}} \quad (14)$$

where \dot{m}_{actual} is obtained experimentally or numerically, d is the inner valve diameter, R is the universal gas constant, γ is the specific heat ratio and T is the temperature.

5.2. Swirl Ratio

The swirl ratio, R_s , is a normalized value used to show the motion pattern of the rotating fluid within the cylinder. Assuming that flow inside the cylinder is a solid body rotational flow, the swirl ratio is obtained by dividing the rotational angular velocity (ω_s) by the crankshaft rotational velocity, as follows (Heywood, 1988)

$$R_s = \frac{\omega_s}{(2\pi N)/60} \quad (15)$$

The direction of swirl ratio is determined according to the right-hand rule. The swirl centre can be the cylinder axis or the centre of mass. For this case, the centre of mass is not located on the cylinder axis, because the piston bowl is not centrally localized. Following the Star-cd (2008), the swirl ratio is computed on the basics of the total angular momentum relative to the centre of mass along the cylinder axis, and the engine speed.

Then, the swirl ratio is computed as

$$R_s = \frac{\sum_{cells} \rho_i V_i [(x_i - x_m) v_i - (y_i - y_m) u_i]}{2\pi \frac{N}{60} I_z} \quad (16)$$

where x_i , y_i and z_i are the centroid coordinates of cell i , x_m , y_m and z_m are the centre of mass coordinates, w_i and v_i are velocity components, ρ_i is the density, V_i is the volume of cell i and I_z is the moment of inertia, which can be computed as follows

$$I_z = \sum_{cells} \rho_i V_i ((y_i - y_m)^2 + (x_i - x_m)^2) \quad (17)$$

6. RESULTS AND DISCUSSION

In order to compare the results produced by the four time steps, the following figures show velocity vectors and pressure fields for a crank angle of 74° after TDC, close to the maximum piston velocity, where it can be verified the extreme situations, regarding the flow complexity. The time period, since the initial condition, is 0.0926667 s, corresponding to an angular interval of 834° (320° – 1154°). The intake valve lift in this moment is 6.839 mm.

Two significant sections are showed, being important to point that the unique difference between these solutions is the time step (same boundary and initial conditions, mesh, wall treatment, differencing schemes, turbulence model, etc.).

The Figs. 3-4 show the velocity vector fields at 1154°, for the time steps of 0.05°, 0.1°, 0.2° and 0.4°, respectively, in the X-Z plane (vertical plane that passes through the valves). At this point, the fluid flow is admitted through helical inlet port, in the form of a strong annular conical jet, where this jet generates regions with different behavior inside the cylinder.

The fluid flow that enters the cylinder induces the creation of a toroidal vortex with counterclockwise. This vortex is further intensified by the flow returning from the piston bowl. Also, it is possible to note the presence of another vortex in the lower right corner, influenced by the main jet.

On the intake valve seat there is a detachment, and also on the intake valve plate, followed by a recirculation. These characteristics of detachment and recirculation flow in the intake valve are confirmed in the literature (Heywood, 1988 ; Ferrari, 2005), as a consequence of the intake valve geometry as the main factor.

Comparing the different time steps, the velocity fields discrepancies are observed only when in the local maximum velocity peak, which it located on the valve seat. For example: the velocity for the time step 0.05° is 108.50 m/s, 0.1° 107.40 m/s, 0.2° 105.50 m/s and 0.4° 105.00 m/s.

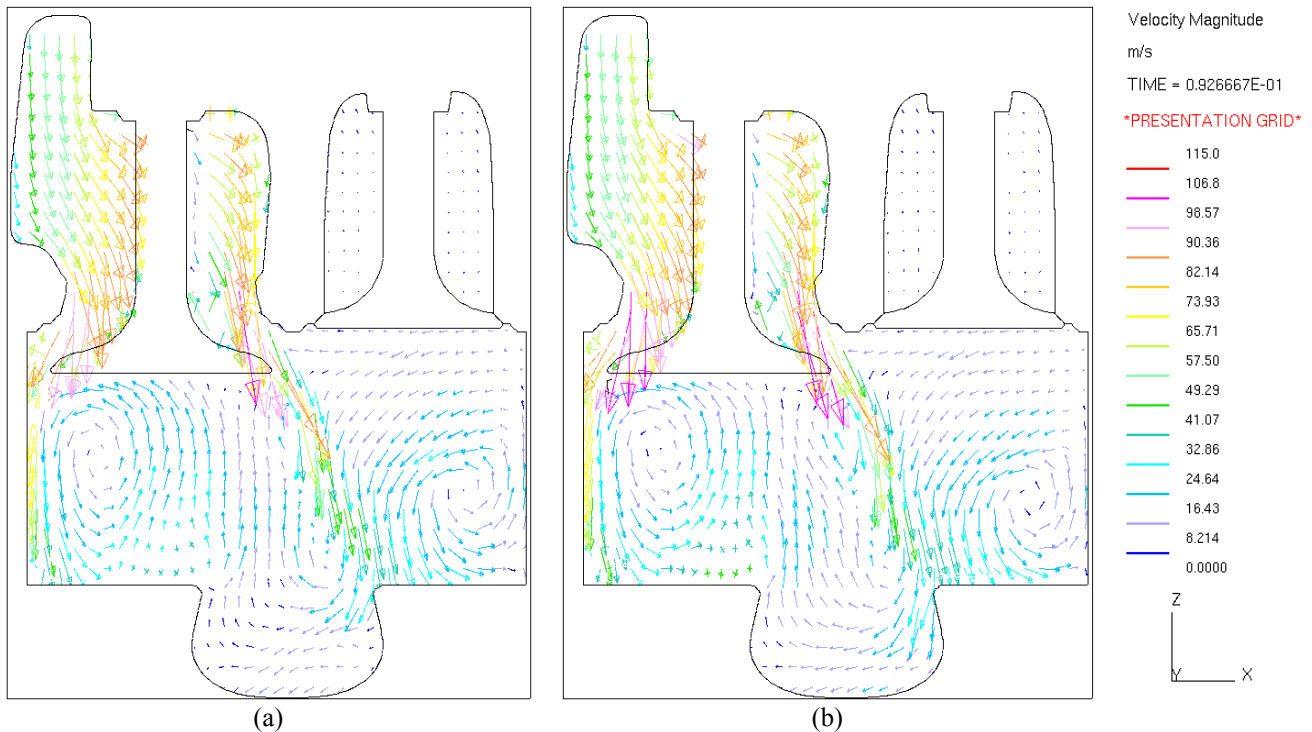


Figure 3. Velocity vectors at 1154°: (a) time step 0.05° , (b) 0.1°

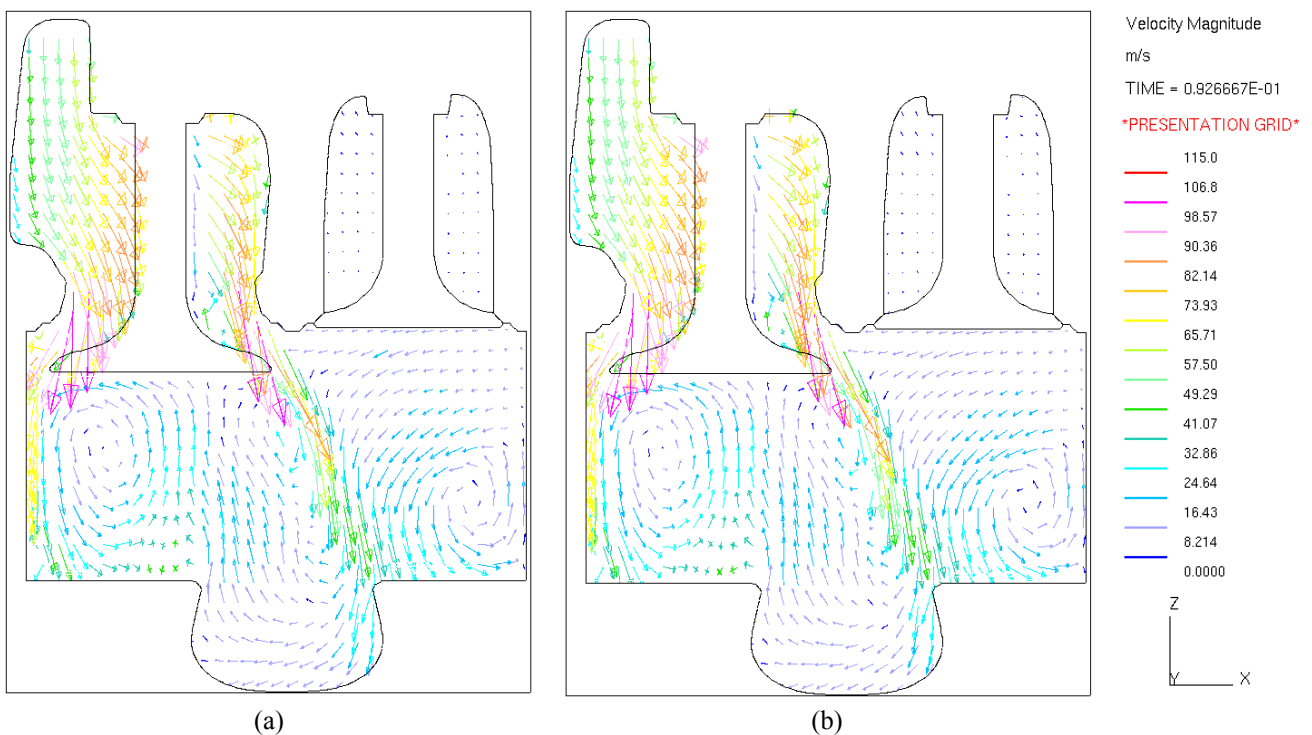


Figure 4. Velocity vectors at 1154°: (a) time step 0.2° , (b) 0.4°

The Figs. 5-6 show the absolute pressure fields in the X-Z plane. It is possible to observe that the lowest values are concentrated around the stem intake valve, because the high velocities and also of cyclone effect, caused by the helical inlet port. Following is a partial regain of pressure inside the cylinder, due to decrease of velocity. This regain increases

when the time step is smaller, showing a dependency of the time step in these solutions, where it is possible to observe that the time step independence has not been achieved yet.

Quantifying the minimum pressure have the following values for 74° after TDC: time de step of 0.05° 91.46 kPa, 0.1° 90.83 kPa, 0.2° 90.51 kPa and 0.4° 90.36 kPa. These differences, although small, can be to noted in the figures.

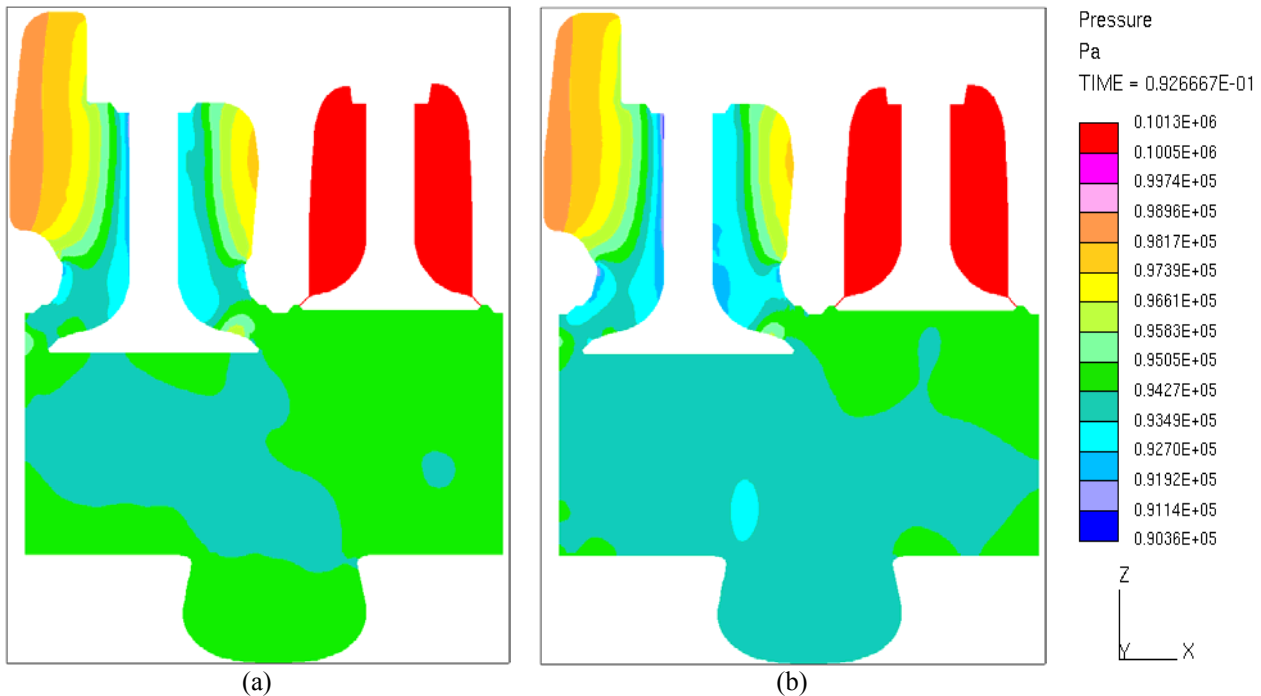


Figure 5. Pressure fields at 1154°: (a) time step 0.05°, (b) 0.1°

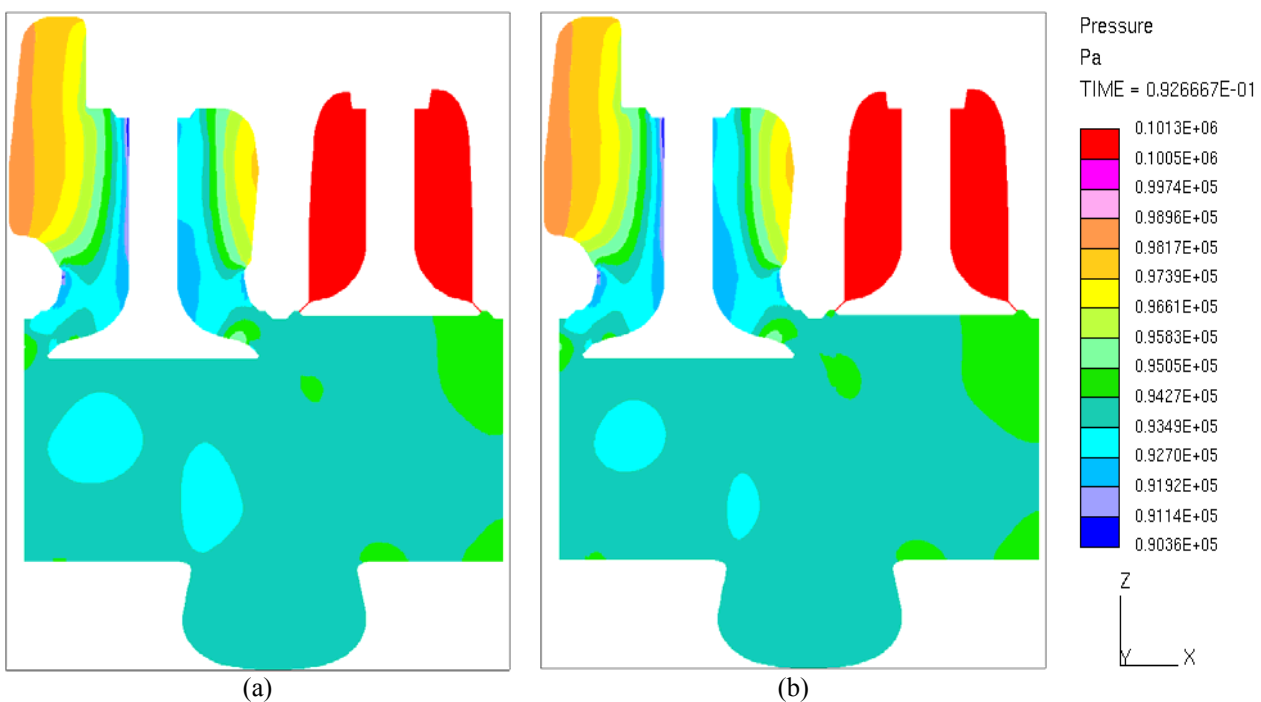


Figure 6. Pressure fields at 1154°: (a) time step 0.2°, (b) 0.4°

The Fig. 7 illustrates the evolution of the discharge coefficient and swirl ratio as a function of the crank angle to the intake stroke. In the first stage of the evolution of discharge coefficient, a strong increase occurs after TDC (1080°), due to the opening of the intake valve, where in this moment the intake pressure port is higher than cylinder pressure. At 1095°, the discharge coefficient value reaches a local peak, and then decreases due to pressure equalization (port-

cylinder). This brief decrease and a subsequent variation of the discharge coefficient can be attributed to the presence of dynamic effects and recirculations in the intake duct.

At 1130°, according to the depression created inside the cylinder by downward piston movement, the cylinder pressure approaches its minimum value, and followed by intake valve open causes a significant increase in discharge coefficient, reaching its maximum value. After, there is a local reduction, due to corresponding increase in cylinder pressure ranging up to intake valve closing.

The result differences between the time steps are more notorious in complex situations; because the smallest time step better captures the dynamic effects.

Regarding the swirl ratio, after TDC its value decreases reaching the minimum at 1095°. The negative value indicates that the resultant of the fluid rotation is clockwise. The swirl ratio reaches its maximum at 1206°, because the strong increase in the discharge coefficient and the considerable intake valve lift, where the counterclockwise flow predominates. The differences between the time steps are small.

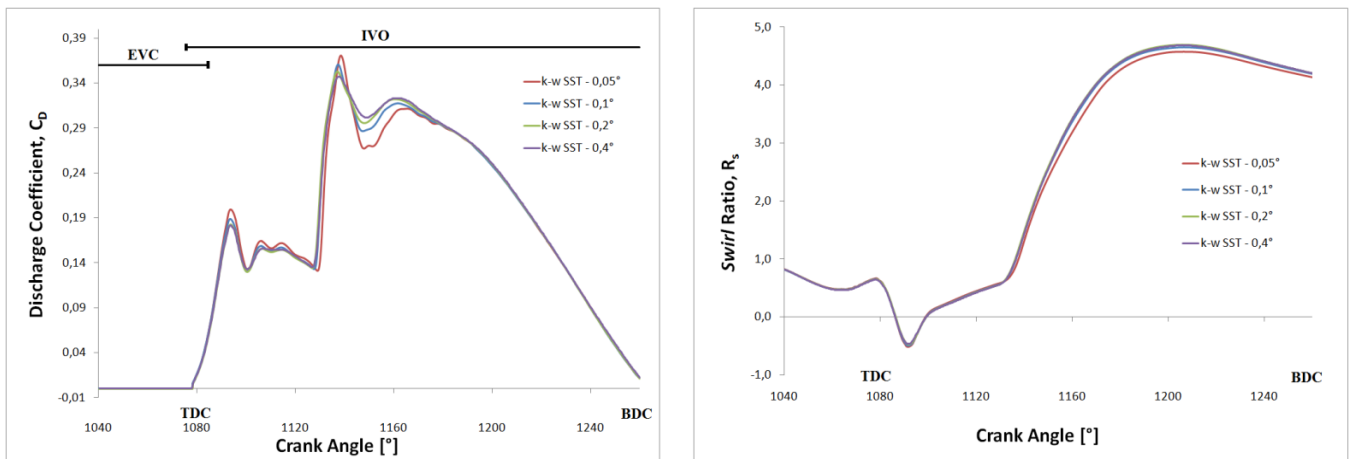


Figure 7. Evolution along crank angle of the discharge coefficient and swirl ratio

The table 1 shows the results for the discharge coefficient and swirl ratio at 1154°. It is possible to note that the value of C_D and R_s increase as the time step increases, possibly due to cylinder pressure decrease to larger Δt . For both parameters are observed the dependence of the results for the time step employed.

Table 1. Comparative parameters at 1154°

Time Step	Discharge Coefficient (C_D)	Swirl Ratio (R_s)	Difference, relative to time step of 0.05° [%]	
			C_D	R_s
0.05°	0.277406	2.723647	-	-
0.1°	0.299806	2.890877	8.07	6.14
0.2°	0.309165	2.943748	11.44	8.08
0.4°	0.310849	2.921623	12.05	7.26

7. CONCLUSIONS

A three-dimensional unsteady turbulent compressible Navier-Stokes solver, Star-cd, was utilized in the present study to investigate the intake and in-cylinder flowfield of a two-valve direct injection compression ignition engine. The following conclusions were found:

- As expected, it is important that a high-quality complete grid be generated to resolve the transient flow processes found during intake stroke. It was very important to have a refined high-quality mesh with minimal skewness and non-uniformity, particularly at the intake port-cylinder interface.
- The comparative parameters presented in the Table 1, the discharge coefficient and swirl ratio, show that there is difference to smallest time step and complex flow situations, for both parameters.
- The presence of recirculations in the port and in-cylinder are detected.
- Analyzing the observed differences between the flow patterns, it is possible to conclude that the presented deviations are sufficient to prejudice a detailed project of the engine internal variable fields, necessary to a correct simulation of reactive flows (combustion).

- New searches need to be developed, aiming to clarify the simulation of the turbulence phenomenon in this kind of complex transient, multidimensional, compressible swirling non-isothermal flow, in movable domain.

8. ACKNOWLEDGEMENTS

The authors thank the financial support from CNPq, Brazil, through a doctoral grant to Zancanaro, F.V.Jr, and scientific productivity grant to Vielmo, H.A. Also, the authors would like to thank the CESUP, RS, Brazil.

9. REFERENCES

- Aita, S., Tabbal, A., Munck, G., Montmayeur, N., Takenaka, Y., Aoyagi, Y., Obana, S., 1991, "Numerical Simulation of Swirling Port-Valve-Cylinder Flow in Diesel Engine", SAE Paper N° 910263.
- Bianchi, G.M., Cantore, G. and Fontanesi, S., 2002a, "Turbulence Modeling in CFD Simulation of ICE Intake Flows: The Discharge Coefficient Prediction", SAE Paper N° 2002-01-1118.
- Bianchi, G.M., Cantore, G., Parmeggiani, P., Michelassi, V., 2002b, "On Application of Nonlinear $k-\varepsilon$ Models for Internal Combustion Engine Flows". Transactions of the ASME vol. 124, pp. 668-677.
- Bianchi, G.M., Fontanesi, S., 2003, "On the Applications of Low-Reynolds Cubic $k-\varepsilon$ Turbulence Models in 3D Simulations of ICE Intake Flows", SAE Paper N° 2003-01-0003.
- Baratta, M., Catania, A.E., Pesce, F.C., Spessa, E., Vielmo, H.A., 2008, "Numerical Analysis of a High Swirl-Generating Helical Intake Port for Diesel Engines". Proceedings of the 12th Brazilian Congress of Thermal Engineering and Sciences, Belo Horizonte, Brazil.
- Baratta, M., Catania, A.E., Pesce, F.C., Spessa, E., Rech, C., Zancanaro, F.V.Jr, Vielmo, H.A., 2009, "Transient Numerical Analysis of a High Swirled Diesel Engine", 20th International Congress of Mechanical Engineering, Gramado – RS, Proceedings of COBEM, Rio de Janeiro, RJ: ABCM.
- Chen, A., Veshagh, A., Wallace, S., 1998, "Intake Flow Predictions of a Transparent DI Diesel Engine", SAE Paper N° 981020.
- Ferrari, G., 2005, "Motori a Combustione Interna", Torino, Ed il Capitello, (in italian).
- Fiat Research Center; Consiglio Nazionale delle Ricerche, 1982, "Motore Monocilindro Diesel con Distribuzione a 2 Valvole e Protezioni Termiche Camera di Combustione", Contract N° 82.00047.93 (in italian).
- Fiat Research Center; Consiglio Nazionale delle Ricerche, 1983, "Metodologia per la Caratterizzazione dei Condotti di Aspirazione Motori in Flusso Stazionario". Contract N° 82.00047.93 (in italian).
- Gosman, A.D., 1985, "Multidimensional Modeling of Cold Flows and Turbulence in Reciprocating Engine", SAE paper N° 850344.
- Heywood, J.B., 1988, "Internal Combustion Engines", McGraw-Hill Inc.
- Hinze, P.O., 1975, "Turbulence", 2nd Edition, McGraw-Hill, New York.
- Hirsch, C., 2007, "Numerical Computational of Internal and External Flows – Vol. II: Computational Methods for Inviscid and Viscous Flows", John Wiley & Sons, New York.
- Huh, K.A., Choi, C.R., Kim, J.G., 1995, "Flow Analysis of the Helical Intake Port and Cylinder of a Direct Injection Diesel Engine", SAE Paper N° 952069.
- Jones, W.P., 1980, "Prediction Methods for Turbulent Flow", Hemisphere, Washington, D.C., pp. 1-45.
- Kurniawan, W.H., Abdullah, S., Shamsudeen, A., 2007, "A Computational Fluid Dynamics Study of Cold-Flow Analysis for Mixture Preparation in a Motored Four-Stroke Direct Injection Engine", Journal of Applied Sciences 7(19): 2710-2724.
- Lakshminarayanan, P.A., Aghav, Y.V., 2010, "Modelling Diesel Combustion", Springer, Mechanical Engineering Serie.
- Menter, F.R., 1993, "Zonal two Equation $k-\omega$ Turbulence Models for Aerodynamic Flows", Proc. 24th Fluid Dynamics Conf., Orlando, Florida, USA, Paper N°. AIAA 93-2906.
- Star-cd, 2008, "User Guides es-ice", CD-adapco.
- Star-cd, 2009, "Methodology", CD-adapco.
- Tindal, M.J., Williams, T.J., Aldoory, M., 1982, "The Effect of Inlet Port Design on Cylinder Gas motion in Direct Injection Diesel Engines", ASME, Flows in Internal Combustion Engines, pp. 101-111.
- Warsi, Z.V.A., 1981, "Conservation Form of the Navier-Stokes Equations in General Nonsteady Coordinates", AIAA Journal, 19, pp. 240-242.
- Wilkes, N.S. and Thompson, C.P., 1983, "An Evaluation of Higher-order Upwind Differencing for Elliptic Flow Problems", CSS 137, AERE, Harwell.

10. RESPONSIBILITY NOTICE

The authors are the only responsible for the printed material included in this paper.